

Graphene p - n junctions with nonuniform Rashba spin-orbit coupling

Marek Rataj^{1,2} and Józef Barnaś¹

¹⁾ *Faculty of Physics, Adam Mickiewicz University, Umultowska 85, 61-614 Poznań, Poland*

²⁾ *The Nano-Bio-Medical Centre, Umultowska 85, 61-614 Poznań, Poland*

Linear conductance of graphene-based p - n junctions with Rashba spin-orbit coupling is considered theoretically. A square potential step is used to model the junctions, while the coupling is introduced in terms of the Kane-Mele model (C.L. Kane and E.J. Mele, Phys.Rev.Lett. 95, 226801(2005)). The main objective is a description of electronic transport in junctions where Rashba parameter is nonuniform. Such a nonuniformity can appear when graphene is asymmetrically covered with atomic layers, or when Rashba coupling is strongly dependent on electric field. It is shown that conductance is significantly modified by the considered nonuniformity, which is most clearly manifested by an anomalous minimum at a certain potential step height.

Owing to the electric field effect¹, various all-graphene-based heterostructures can be easily made by means of electrostatic gates. The simplest structures of this kind are p - n junctions, which have been already analysed theoretically² and investigated experimentally³. Generally, transport characteristics of such junctions significantly depend on the spin-orbit interactions in graphene⁴⁻⁶. This is mainly due to the fact that according to the commonly used Kane-Mele model⁷, the intrinsic coupling opens a band gap, while the Rashba coupling (RSOC) splits both the conduction and valence bands. In this paper we focus on the latter, motivated by recent results showing that it can be made significantly dominant in graphene, as pointed out in Refs. 12–18, where RSOC parameters of the order of 10 meV were reported.

The parameter of RSOC has been so far treated in transport investigations as a constant throughout the structure and also independent of the gate voltages used to make p - n junctions^{4,5}. However, this parameter can be generally nonuniform, which may occur when graphene is covered with an atomic layer from bottom in one part of the junction and on top in the second part¹²⁻¹⁸, or when RSOC is strongly dependent on electric field⁸⁻¹⁰. This problem is addressed in the present paper, where we show that conductance of such p - n junctions differs from that of junctions with constant spin-orbit coupling. We focus especially on a situation in which the RSOC parameter changes sign at the border between the two parts of the junction. All this gives rise to anomalous behaviour of the corresponding conductance.

In order to describe charge carriers in graphene we employ the effective low-energy Hamiltonian¹¹, $H_0 = -i\hbar v_F(\sigma_x \partial_x + \sigma_y \partial_y) \otimes s_0$, where v_F is the electron velocity. We use the notation with σ_α and s_α being the Pauli matrices (for $\alpha = x, y, z$) in the pseudospin and spin spaces, respectively, and σ_0 and s_0 denoting the corresponding unit matrices. We restrict our considerations to a single electronic valley, neglecting thus any inter-valley scattering. RSOC is taken in the form introduced by Kane and Mele⁷, $H_R = \lambda(\sigma_x \otimes s_y - \sigma_y \otimes s_x)$, where λ is the coupling parameter. The full Hamiltonian,

$H = H_0 + H_R$, has the following eigenvalues:

$$E = l\lambda + s\sqrt{\lambda^2 + (k_x^2 + k_y^2)v_F^2\hbar^2}, \quad (1)$$

where \mathbf{k} is the two-dimensional wave vector, $s = 1$ ($s = -1$) for the conduction (valence) band, and $l = \pm 1$ is used to distinguish between the two subbands.

The p - n junction is described by the term, $V(x, y) = V_0\Theta(x)\sigma_0 \otimes s_0$, to be added to the full Hamiltonian. Let us denote the Fermi energy (measured from the neutrality point in the left part of the junction) by E_F .

Assume now a particle of energy E at the Fermi level, $E = E_F$, in the subband l is incident on the potential step at an arbitrary angle ϕ . The corresponding wave function has the form of a plane wave multiplied by a column vector derived in Ref. 4, $\psi_{E,\phi,l}^i(x, y) = |sk_x, E, \phi, l\rangle \exp[i sk_x x] \exp[i k_y y] \equiv \psi_{E,\phi,l}^i(x) \exp[i k_y y]$, where k_x is a positive solution of Eq. (1) (note s ensures that group velocity points in the right direction). In the same way one can build the wave functions for carriers reflected and transmitted into the subband l ; $r_l \psi_{E,\phi,l}^r(x, y)$ and $t_l \psi_{E-V_0,\phi,l}^t(x, y)$, and for carriers reflected and transmitted into the other subband, $l' \neq l$; $r'_l \psi_{E,\phi,l'}^r(x, y)$ and $t'_l \psi_{E-V_0,\phi,l'}^t(x, y)$. Here, r_l , t_l , r'_l and t'_l are the corresponding reflection and transmission amplitudes. Owing to the translational symmetry along the y direction, the k_y component of the wave vector is conserved.

To find the linear conductance we need to know the amplitudes t_l and t'_l , which can be found from the continuity condition at the boundary $x = 0$,

$$\begin{aligned} \psi_{E,\phi,l}^i(x=0) + r_l \psi_{E,\phi,l}^r(x=0) + r'_l \psi_{E,\phi,l'}^r(x=0) \\ = t_l \psi_{E-V_0,\phi,l}^t(x=0) + t'_l \psi_{E-V_0,\phi,l'}^t(x=0). \end{aligned} \quad (2)$$

Having found the transmission amplitudes and taking also into account the respective group velocities, one obtains the corresponding transmission probabilities T_l and T'_l . The full linear conductance can be then obtained by integrating over all incidence angles,

$$G = \frac{2k_F e^2 W}{\pi \hbar} \int d\phi \sum_l \frac{k_F^{(l)}}{k_F} (T_l + T'_l) \cos(\phi). \quad (3)$$

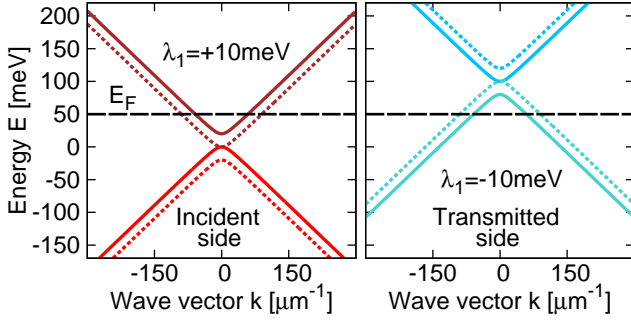


FIG. 1. Band structure of graphene for $|\lambda_1| = 10$ meV, $\alpha^{-1} = 0$, $E_F = 50$ meV, and $V_0 = 100$ meV. Left part shows the spectrum on the incident side of the junction (where $\lambda_1 = 10$ meV), while the right part shows the spectrum on the transmitted side (where $\lambda_1 = -10$ meV). The solid (dotted) lines distinguish subband with opposite index l .

In the following, the conductance will be normalized to the factor G_0 defined as $G_0 = 2e^2 W k_F / (h\pi)$, where k_F is an average of incident Fermi wave vectors $k_F^{(l)}$, while e is the electron charge and W is the sample width.

The RSOC parameter λ can in general be separated into two terms; $\lambda = \lambda_1 + \lambda_2(\mathbf{E})$. The first term is independent of electric field – it may be due to the adjacent atomic layers (substrate/cover layers). The second term can be controlled by external electric field \mathbf{E} (gate voltages), $\lambda_2(\mathbf{E}) = \alpha_1 \mathbf{z} \cdot \mathbf{E}$, where \mathbf{z} is a unit vector perpendicular to the graphene plane, and α_1 is a relevant parameter. The Fermi level in graphene is also controlled by electric field, and this dependence can be expressed as $\tilde{E}_F = \text{sign}(\mathbf{z} \cdot \mathbf{E}) \sqrt{|\mathbf{z} \cdot \mathbf{E}|} \alpha_2$, where α_2 is a parameter, while $\tilde{E}_F = E_F$ for $x < 0$ and $\tilde{E}_F = E_F - V_0$ for $x > 0$. Thus, when the Fermi level is tuned by the gate voltage, the RSOC parameter λ has to be adjusted according to the formula

$$\lambda = \lambda_1 + \text{sign}(\tilde{E}_F) \alpha^{-1} \tilde{E}_F^2, \quad (4)$$

where $\alpha = \alpha_2^2 / \alpha_1$. In the following we will consider two options for the sign reversal of the RSOC parameter at the potential step. First situation is when $\alpha^{-1} = 0$ and λ_1 is positive on one side of the step and negative on the other side. The second possibility appears when α^{-1} is sufficiently large, while λ_1 is small (we take $\lambda_1 = 0$ for clarity of the argument) and constant through the structure. We begin with the former.

In Fig. 1 we show the band structure of graphene on the two sides of the junction for $|\lambda_1| = 10$ meV. The assumed value is typical for graphene covered by atomic planes^{12–18}. The parameter λ_1 is positive on the incident side and negative on the transmitted one (an opposite case would be fully symmetrical). Note, that apart from an up-shift, the spectrum on the transmitted side is inverted with respect to that on the incident side. This inversion is due to the sign reversal of the RSOC parameter λ_1 at the potential step.

Figure 2 shows how the corresponding conductance G

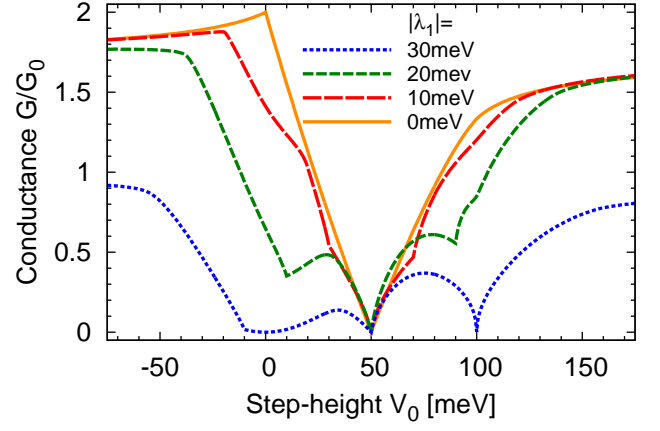


FIG. 2. Normalized conductance versus potential step height V_0 for $|\lambda_1|$ as indicated, with λ_1 positive on the incidence side and negative on the transmitted side. The other parameters are as in Fig.1

depends on the potential step height V_0 for four different values of $|\lambda_1|$. The curve corresponding to $\lambda_1 = 0$ serves as a reference. For the two curves corresponding to the lower values of $|\lambda_1| \neq 0$ the incident carriers come from both conduction subbands (as in the case shown in Fig. 1). Therefore the corresponding conductance reaches values above $G/G_0 = 1$. There is a general trend in these curves that, when V_0 moves from the global minimum at 50 meV towards larger values, the conductance grows until it saturates, similarly to the $|\lambda_1| = 0$ case. When V_0 moves towards lower values in turn, the conductance also grows at first and finally saturates, but the maximum present for $\lambda_1 = 0$ at $V_0 = 0$ is suppressed. This reduction is due to band mismatch created by inverted band splitting on both sides of the junction. Moreover, in general Fermi level on the transmitted side crosses either one or two subbands. The point, where a new subband enters (or leaves) the conduction regime is associated with a kink in the conductance curve. The curve for $|\lambda_1| = 30$ meV differs from the others. First of all it reaches values only up to $G/G_0 = 1$, since the carriers on the incident side come from only one subband. Moreover, at $V_0 = 0$ the aforementioned band mismatch leads to a minimum equal zero. Furthermore, only one of the kinks mentioned above is visible in this case (at $V_0 = -10$ meV). Finally, at $V_0 = 100$ meV an anomalous conductance minimum occurs.

Consider now the second situation, in which the RSOC parameter is dependent on electric field, and let us assume the simplest case where $\lambda_1 = 0$. In Fig. 3 we show the band structure of graphene on the incident and transmitted sides of the junction for indicated values of the step height V_0 . Since the RSOC depends on the gate voltages (and therefore on the Fermi level and V_0), for each situation the RSOC parameter is adjusted according to the formula (4). This dependence can also lead to sign reversal of the RSOC parameter at the potential step. To emphasize this effect, we assumed α^{-1} significantly

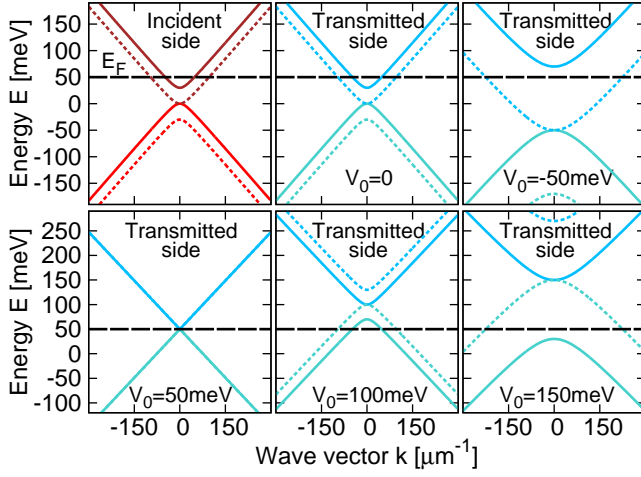


FIG. 3. Band structure of graphene for $\lambda_1 = 0$, $\alpha = 0.25$ eV, $E_F = 50$ meV, and for indicated values of the potential step height V_0 . Part (a) shows the spectrum on the incident (left) side of the junction, while the parts (b) to (f) show spectra on the transmitted (right) side for V_0 as indicated.

larger than currently available data for graphene¹⁰. But one may expect, that this parameter can be increased by means of an appropriate substrate and/or cover layers.

In Fig. 4 we present how the conductance G depends on the potential step height V_0 for different values of α . The first three curves (corresponding to larger values of α) show similar behaviour, since in all these cases the incident carriers come from both conduction subbands. First, there is a minimum at $V_0 = 50$ meV, corresponding to vanishing density of states on the transmitted side (RSOC vanishes as well, see Fig. 3(d)). When V_0 increases from this value, the conductance grows until it reaches a maximum value larger than $G/G_0 = 1$, and then it suddenly drops. This drop occurs when one of the subbands on the transmitted side ceases taking part in conduction (transition from (e) to (f) in Fig. 3). When V_0 changes from $V_0 = 50$ meV towards lower values, the normalized conductance grows until it reaches a maximum value, $G/G_0 = 2$, which is located at $V_0 = 0$ (no potential step, see (a) and (b) in Fig. 3). When V_0 goes further to negative values, there is a drop in conductance of the same origin as the one discussed above.

The curve for $\alpha = 0.08$ eV in Fig. 4 corresponds to the case where the incident carriers come from one subband only. Therefore, the conductance is always equal to or smaller than G_0 , $G/G_0 \leq 1$. As before, there is a maximum at $V_0 = 0$ and a minimum at $V_0 = 50$ meV. Additionally, an anomalous minimum appears at $V_0 = 100$ meV. This anomalous minimum is of the same nature as the one discussed in the case where $\alpha^{-1} = 0$.

In summary, we have considered the charge transport through p - n junctions in graphene with nonuniform RSOC parameter. The nonuniformity was either due to asymmetric location of adjacent atomic planes (on top in one part of the junction and at bottom in the other part),

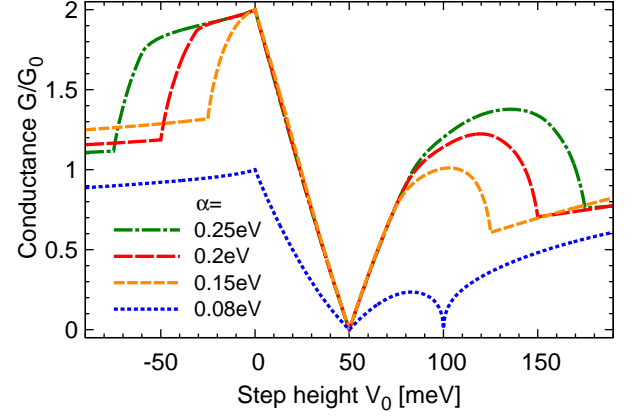


FIG. 4. Normalized conductance versus potential step height V_0 for $\lambda_1 = 0$, $E_F = 50$ meV and indicated values of the parameter α .

or due to a strong dependence of the RSOC parameter on electric field (and thus on the gate voltage used to generate carriers). We have especially focused on the situation when the RSOC parameter changes sign at the potential step. We have found a suppression of the conductance at characteristic points, which is a consequence of the inverted band splitting by RSOC.

Acknowledgements The research has been carried out under the project co-financed by European Union from European Regional Fund within Operational Programme Innovative Economy.

- ¹K. S. Novoselov, A. K. Geim, S. V. Morozov, D. Jiang, Y. Zhang, S. V. Dubonos, I. V. Grigorieva, and A. A. Firsov, *Science* **306**, 666 (2004).
- ²M. I. Katsnelson, K. S. Novoselov, and A. K. Geim, *Nature Physics* **2**, 620 (2006).
- ³M. C. Lemme, T. J. Echtermeyer, M. Baus, and H. Kurz, *Electron Device Letters, IEEE* **28**, 282 (2007).
- ⁴A. Yamakage, K. I. Imura, J. Cayssol, and Y. Kuramoto, *Europhys. Lett.* **87**, 47005 (2009).
- ⁵A. Yamakage, K.-I. Imura, J. Cayssol, and Y. Kuramoto, *Phys. Rev. B* **83**, 125401 (2011).
- ⁶C. Bai, J. Wang, J. Tian, and Y. Yang, *Physica E* **43**, 207 (2010).
- ⁷C. L. Kane and E. J. Mele, *Phys. Rev. Lett.* **95**, 226801 (2005).
- ⁸D. Huertas-Hernando, F. Guinea, and A. Brataas, *Phys. Rev. B* **74**, 155426 (2006).
- ⁹H. Min, J. E. Hill, N. A. Sinitsyn, B. R. Sahu, L. Kleinman, and A. H. MacDonald, *Phys. Rev. B* **74**, 165310 (2006).
- ¹⁰M. Gmitra, S. Konschuh, C. Ertler, C. Ambrosch-Draxl, and J. Fabian, *Phys. Rev. B* **80**, 235431 (2009).
- ¹¹P. R. Wallace, *Physical Review* **71**, 622 (1947).
- ¹²A. Varykhalov, J. Sánchez-Barriga, A. M. Shikin, C. Biswas, E. Vescovo, A. Rybkin, D. Marchenko, and O. Rader, *Phys. Rev. Lett.* **101**, 157601 (2008).
- ¹³J. Sánchez-Barriga, A. Varykhalov, M. Scholz, O. Rader, D. Marchenko, A. Rybkin, A. Shikin, and E. Vescovo, *Diamond Relat. Mater.* **19**, 734 (2010).
- ¹⁴E. I. Rashba, *Phys. Rev. B* **79**, 161409 (2009).
- ¹⁵Z. Y. Li, Z. Q. Yang, S. Qiao, J. Hu, and R. Q. Wu, *J. Phys.: Condens. Matter* **23**, 225502 (2011).
- ¹⁶A. H. Castro Neto and F. Guinea, *Phys. Rev. Lett.* **103**, 026804 (2009).
- ¹⁷C. Ertler, S. Konschuh, M. Gmitra, and J. Fabian, *Phys. Rev. B* **80**, 041405 (2009).

¹⁸Y. S. Dedkov, M. Fonin, U. Rüdiger, and C. Laubschat, Phys. Rev. Lett. **100**, 107602 (2008).